

Cationic Cyclometalated Iridium Luminophores: Photophysical, Redox, and Structural Characterization

Francesco Neve,^{*,†} Massimo La Deda,[†] Alessandra Crispini,[†] Anna Bellusci,[†]
Fausto Puntoriero,[‡] and Sebastiano Campagna^{*,‡}

*Dipartimento di Chimica, Università della Calabria, I-87030 Arcavacata di Rende (CS), Italy,
and Dipartimento di Chimica Inorganica, Chimica Analitica e Chimica Fisica,
Università di Messina, Via Sperone 31, I-98166 Messina, Italy*

Received July 7, 2004

The photophysical and electrochemical properties of a series of cationic cyclometalated Ir(III) complexes is reported. The complexes are of general formula $[\text{Ir}(\text{ppy})_2(\text{R},\text{R}'\text{-bpy})]^+$ (**1–5**; PF_6^- as counterion) where ppy = 2-phenylpyridinato anion. Complexes **1–3** contain asymmetric bpy ligands with R and R' substituents in the 6' and 4' positions, while complexes **4** and **5** bear bpy ligands symmetrically substituted in the 4 and 4' positions. Complex **5** was structurally characterized by single-crystal X-ray crystallography, revealing a *cis* arrangement of the metalated C atoms of the ppy ligands. All the species exhibit strong absorption in the UV region, due to spin-allowed ligand-centered (LC) transitions, and moderately intense bands in the visible region, due to charge transfer (CT) transitions. Several redox processes have been evidenced in each complex and assigned to specific components. The complexes also exhibit relatively strong and long-lived (from 10^{-8} to 10^{-5} s, depending on temperature and matrix) luminescence, in all the experimental conditions used (acetonitrile solution and spin-coated films at 298 K; butyronitrile rigid matrix at 77 K). The substituents of the polypyridine ligands affect in a substantial way the redox and photophysical properties of the compounds. In particular, a phenyl substituent on the polypyridine chelating ligand in the 6' position (complexes **1–3**) stabilizes oxidation of an orbital which receives significant contributions from the ppy ligands and leads to emission from triplet ligand-to-ligand charge transfer (LLCT) excited states. When such a phenyl is absent in the ligand structure (complexes **4** and **5**), the usual triplet metal-to-ligand charge transfer (MLCT) emission predominates.

Introduction

The interest in photophysical and redox properties of Ir(III) cyclometalated compounds is increasing at an exponential rate. In addition to fundamental reasons, also powered by potential applications in the field of solar energy conversion, which stimulated interest in the field in the last two decades, the excited state properties of Ir(III) cyclometalated compounds have indeed experienced a blooming attraction in the past few years, as these species are extremely promising to play the role of active components (i.e., the emissive species) in organic light-emitting diodes (OLED).^{1,2}

Ir(III) cyclometalated species fit well many requisites for the preparation of OLED. (i) They exhibit luminescence from their lowest-lying (formally) triplet metal-to-ligand charge transfer (MLCT) state; this overcomes the limitation of the upper 0.25 efficiency in light emission by organic fluorophores, due to the spin states

involved. (ii) The wavelength of emitted light can be tuned over a large spectral range, as a consequence of the possibility offered by a clever choice and combination of ligands and ligand substituents. (iii) Emission quantum yields are relatively high in both fluid solution and solid state, often even higher than those exhibited by similar complexes based on different transition metals, including the most famous Ru(II) polypyridine complexes.

Presently, two different synthetic strategies are considered in light of improving the photoluminescent (and electroluminescent) properties and the processibility of the Ir-based phosphorescent emitters. One group of molecules refers to the parent species *fac*- $[\text{Ir}(\text{ppy})_3]$ (ppy = 2-phenylpyridinato anion),³ while the other considers bis-cyclometalated Ir species like $[\text{Ir}(\text{ppy})_2(\text{acac})]$ (acac = acetylacetonate ion) or analogues.⁴ In both cases, the targeted end-product is a neutral, six-coordinate Ir(III) species. From a synthetic point of view, tuning of intrinsic luminescence and quantum efficiency (preliminary to the final power efficiency of the electroluminescent device) has been achieved through chemi-

* To whom correspondence should be addressed. E-mail: f.neve@unical.it or photochem@chem.unime.it.

[†] Università della Calabria.

[‡] Università di Messina.

(1) (a) Kohler, A.; Wilson, J. S.; Friend, R. H. *Adv. Mater.* **2002**, *14*, 701. (b) Maestri, M.; Balzani, V.; Deuschel-Cornioley, C.; von Zelewsky, A. *Adv. Photochem.* **1992**, *17*, 1.

(2) (a) Baldo, M. A.; Lamansky, S.; Burrows, P. E.; Thompson, M. E.; Forrest, S. R. *Appl. Phys. Lett.* **1999**, *75*, 4. (b) Baldo, M. A.; Thompson, M. E.; Forrest, S. R. *Nature* **2000**, *403*, 750.

(3) King, K. A.; Spellane, P. J.; Watts, R. J. *J. Am. Chem. Soc.* **1985**, *107*, 1431.

(4) Lamansky, S.; Djurovich, P.; Murphy, D.; Abdel-Razzaq, F.; Kwong, R.; Tsyba, I.; Bortz, M.; Mui, R.; Bau, R.; Thompson, M. E. *Inorg. Chem.* **2001**, *40*, 1704.

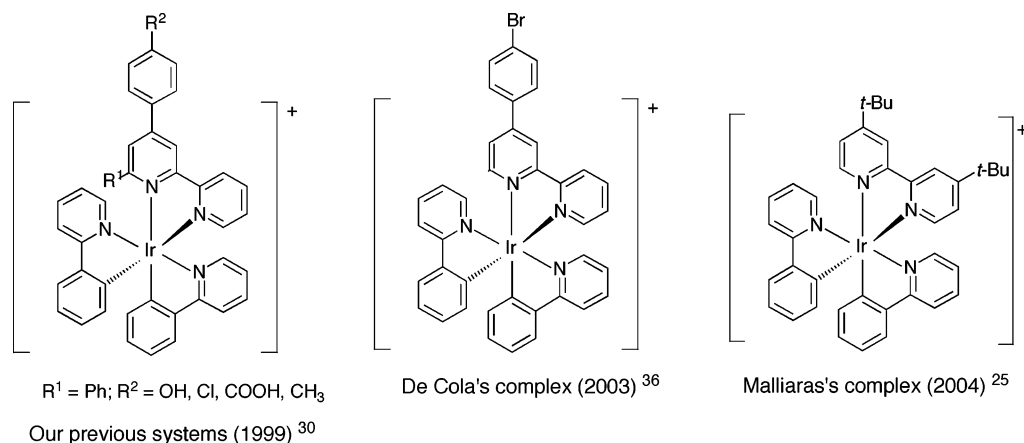


Figure 1. Selected cationic cyclometalated Ir(III) complexes with substituted 2,2'-bipyridine ligands.

cal modification of the cyclometalating moieties in the case of homoleptic Ir(III) complexes.^{5–12} For the more versatile mixed-ligand $[\text{Ir}(\text{C}\wedge\text{N})_2(\text{L})]$ species, modifications can occur either in the cyclometalated C \wedge N part or in the ancillary anionic L ligand.^{13–19}

Recently,²⁰ the species $[\text{Ir}(\text{btp})_2(\text{acac})]$ ¹³ (btp = 2-(2'-benzothienyl)pyridinato) has found application as a phosphorescent dopant in the fabrication of polymer light-emitting electrochemical cells (LEC),²¹ a type of electroluminescent device that already represents an alternative to traditional organic LEDs. In a more simplified version, LECs may use pure ionic transition metal complexes that supply emission centers and ionic conductivity in the same species.^{22–24} Bridging the gap of Ir-based OLEDs and transition metal-based LECs,

Malliaras and co-workers²⁵ have timely reported on the use of a cationic cyclometalated Ir(III) complex for the preparation of a single-layer electroluminescent device. The complex, $[\text{Ir}(\text{ppy})_2(\text{dtb-bpy})][\text{PF}_6]$ (dtb-bpy = 4,4'-di-*tert*-butyl-2,2'-bipyridine), belongs to the well known family of emissive Ir(III) mononuclear complexes containing the $[\text{Ir}(\text{ppy})_2(\text{bpy})]^+$ core.^{26–36} Previous studies from our group have shown that cationic bis-cyclometalated $[\text{Ir}(\text{ppy})_2(\text{R},\text{R}'\text{-bpy})]^+$ (R = Ph; R' = 4''-X-Ph, X = OH, CH₃, COOH, Cl) complexes containing ancillary bipyridine ligands substituted in the 4' and 6' positions (Figure 1) are quite good emitters from triplet metal-to-ligand charge transfer (³MLCT) excited states with partial contribution from σ bond-to-ligand charge transfer (SBLCT) ones, also designated as ligand-to-ligand charge transfer (LLCT) states.^{30,31} Here we present results on the electrochemical and photophysical properties of another family of $[\text{Ir}(\text{ppy})_2(\text{R},\text{R}'\text{-bpy})]^+$ species that can be divided into two subgroups. The first contains the bpy ligand with dissimilar R and R' substituents in the 4' and 6' positions, while the other refers to complexes where the bpy bears equal substituents in the 4 and 4' position (Figure 2). In general, R and R' are long-tailed substituents of low polarity. For both subgroups, the introduction of such substituents had the scope (among others) of imparting to the resulting complexes higher solubility in organic media

(5) (a) Grushin, V. V.; Herron, N.; LeCloux, D.; Marshall, W. J.; Petrov, V. A.; Wang, Y. *Chem. Commun.* **2001**, 1494. (b) Wang, Y.; Herron, N.; Grushin, V. V.; LeCloux, D.; Petrov, V. A. *Appl. Phys. Lett.* **2001**, *79*, 449.

(6) Xie, H. Z.; Liu, M. W.; Wang, O. W.; Zhang, X. H.; Lee, C. S.; Hung, L. S.; Lee, S. T.; Teng, P. F.; Kwong, H. L.; Zheng, H.; Che, C. M. *Adv. Mater.* **2001**, *13*, 1245.

(7) Gong, X.; Robinson, M. R.; Ostrowski, J. C.; Moses, D.; Bazan, G. C.; Heeger, A. J. *Adv. Mater.* **2002**, *14*, 581.

(8) Ostrowski, J. C.; Robinson, M. R.; Heeger, A. J.; Bazan, G. C. *Chem. Commun.* **2002**, 784.

(9) (a) Lo, S.-C.; Male, N. A. H.; Markham, J. P. J.; Magennis, S. W.; Burn, P. L.; Salata, O. V.; Samuel, I. D. W. *Adv. Mater.* **2002**, *14*, 975. (b) Lo, S.-C.; Namdas, E. B.; Burn, P. L.; Samuel, I. D. W. *Macromolecules* **2003**, *36*, 9721.

(10) Gong, X.; Ostrowski, J. C.; Bazan, G. C.; Moses, D.; Heeger, A. J.; Liu, M. S.; Jen, A. K.-Y. *Adv. Mater.* **2003**, *15*, 45.

(11) Zhu, W.; Liu, C.; Su, L.; Yang, W.; Ming, Y.; Cao, Y. *J. Mater. Chem.* **2003**, *13*, 50.

(12) Beeby, A.; Bettington, S.; Samuel, I. D. W.; Wang, Z. *J. Mater. Chem.* **2003**, *13*, 80.

(13) Lamansky, S.; Djurovich, P.; Murphy, D.; Abdel-Razzaq, F.; Lee, H.-E.; Adachi, C.; Burrows, P. E.; Forrest, S. R.; Thompson, M. E. *J. Am. Chem. Soc.* **2001**, *123*, 4304.

(14) D'Andrade, B. W.; Thompson, M. E.; Forrest, S. R. *Adv. Mater.* **2002**, *14*, 147.

(15) D'Andrade, B. W.; Brooks, J.; Adamovich, V.; Thompson, M. E.; Forrest, S. R. *Adv. Mater.* **2002**, *14*, 1032.

(16) Tsuzuki, T.; Shirasawa, N.; Suzuki, T.; Tokito, S. *Adv. Mater.* **2003**, *15*, 1455.

(17) Nazeeruddin, Md. K.; Humphry-Baker, R.; Berner, D.; Rivier, S.; Zuppiroli, L.; Graetzel, M. *J. Am. Chem. Soc.* **2003**, *125*, 8790.

(18) Chen, X.; Liao, J.-L.; Liang, Y.; Ahmed, M. O.; Tseng, H.-E.; Chen, S.-A. *J. Am. Chem. Soc.* **2003**, *125*, 636.

(19) Yang, C.-H.; Tai, C.-C.; Sun, I.-W. *J. Mater. Chem.* **2004**, *14*, 947.

(20) Chen, F.-C.; Yang, Y.; Pei, Q. *Appl. Phys. Lett.* **2002**, *81*, 4278.

(21) (a) Pei, Q.; Yu, G.; Zhang, C.; Yang, Y.; Heeger, A. J. *Science* **1995**, *269*, 1086. (b) deMello, J. C.; Tessler, N.; Graham, S. C.; Friend, R. H. *Phys. Rev. B* **1998**, *57*, 12951.

(22) Gao, F. G.; Bard, A. J. *J. Am. Chem. Soc.* **2000**, *122*, 7426.

(23) Welter, S.; Brunner, K.; Hofstraat, J. W.; De Cola, L. *Nature* **2003**, *421*, 54.

(24) For a review of LECs based on transition metal complexes, see: Slinker, J.; Bernards, D.; Houston, P. L.; Abruna, H.; Bernhard, S.; Malliaras, G. G. *Chem. Commun.* **2003**, 2392.

(25) Slinker, J. D.; Gorodetsky, A. A.; Lowry, M. S.; Wang, J.; Parker, S.; Rohl, R.; Bernhard, S.; Malliaras, G. G. *J. Am. Chem. Soc.* **2004**, *126*, 2763.

(26) Ohsawa, Y.; Sprouse, S.; King, K. A.; DeArmond, M. K.; Hanck, K. W.; Watts, R. J. *J. Phys. Chem.* **1987**, *91*, 1047.

(27) Garces, F. O.; King, K. A.; Watts, R. J. *Inorg. Chem.* **1988**, *27*, 3464.

(28) Wilde, A. P.; Watts, R. J. *J. Phys. Chem.* **1991**, *95*, 622.

(29) Colombo, M. G.; Hauser, A.; Güdel, H. U. *Inorg. Chem.* **1993**, *32*, 3088.

(30) Neve, F.; Crispini, A.; Campagna, S.; Serroni, S. *Inorg. Chem.* **1999**, *38*, 2250.

(31) Neve, F.; Crispini, A.; Loiseau, F.; Campagna, S. *Dalton Trans.* **2000**, 1399.

(32) Neve, F.; Crispini, A.; Serroni, S.; Loiseau, F.; Campagna, S. *Inorg. Chem.* **2001**, *40*, 1093.

(33) Lo, K. K.-W.; Ng, D. C.-M.; Chung, C. K. *Organometallics* **2001**, *20*, 4999.

(34) Lo, K. K.-W.; Chung, C. K.; Ng, D. C.-M.; Zhu, N. *New J. Chem.* **2002**, *26*, 81.

(35) Lo, K. K.-W.; Chung, C. K.; Zhu, N. *Organometallics* **2003**, *22*, 475.

(36) Plummer, E. A.; Hofstraat, J. W.; De Cola, L. *Dalton Trans.* **2003**, 2080.

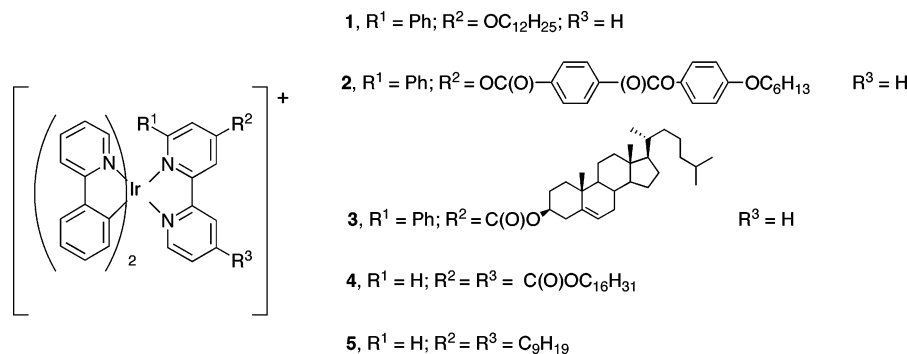


Figure 2. Schematic structures of Ir(III) complexes 1–5.

and, therefore, better processibility of the expected films. Moreover, the long-tailed substituents can also decrease intermolecular interactions in the solid state, which could lead to excited state self-quenching, a poisoning process for electroluminescent devices.

Results and Discussion

Synthetic Studies. The preparation of the mononuclear complexes 1–5 was carried out through bridge splitting reactions of the dinuclear precursor $[\text{Ir}(\text{ppy})_2\text{Cl}]_2$ ³⁷ with the appropriate bipyridine ligand in stoichiometric amount.³⁰ In this regard, our method guarantees the formation of $[\text{Ir}(\text{ppy})_2(\text{R},\text{R}'\text{-bpy})]^+$ species in rather mild conditions, if compared to other synthetic procedures that require harsher conditions (reflux in a high-boiling solvent mixture) and much longer reaction times.²⁵ In our case, lesser decomposition, limited work-up, and good yields are undoubtable advantages that testify a well-established procedure.^{17,31–33,35,36} While the synthesis of compounds 1–3 was reported earlier,³⁸ compounds 4 and 5 were prepared on purpose for this study. The new species were obtained as PF_6^- salts and characterized through spectroscopic and spectrometric methods in addition to elemental analysis. The MALDI-TOF mass spectra of 4 and 5 confirmed the successful formation of the desired complexes and their remarkable stability during the desorption/ionization process.¹ ^1H NMR spectroscopic results confirmed that the complexes are always in pure stereoisomeric form (one set of proton signals). The proposed coordination at the metal center is the one containing ppy ligands with *cis* metalated carbons and *trans* nitrogen atoms, as revealed by previous structural studies on mononuclear species containing the $\{\text{M}(\text{C}\wedge\text{N})_2\}$ fragment ($\text{M} = \text{Ir},^{4,30,35,38–41} \text{Rh}^{42,43}$). Our prediction was confirmed by a single-crystal X-ray analysis of 5.

Crystal Structure of Complex 5. Complex 5 crystallizes in the monoclinic $C2/c$ space group with centrosymmetric cations and centrosymmetric hexafluorophosphate anions. A perspective view of the cation is

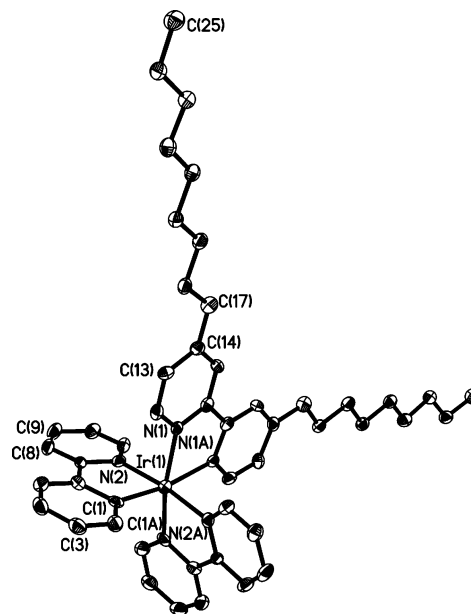


Figure 3. Perspective view of the complex cation of 5 with atomic numbering scheme (ellipsoids at the 50% level). Hydrogen atoms are omitted for clarity.

Table 1. Selected Bond Lengths (Å) and Angles (deg) for Complex 5

Ir(1)–C(1)	2.015(7)	Ir(1)–N(2)	2.057(6)
Ir(1)–N(1)	2.151(6)	Ir(1)–N(1A)	2.151(6)
Ir(1)–C(1A)	2.015(7)	Ir(1)–N(2A)	2.057(6)
N(1)–Ir(1)–N(2)	89.9(2)	N(1)–Ir(1)–N(1A)	76.3(3)
N(2)–Ir(1)–N(1A)	95.9(2)	C(1)–Ir(1)–N(1A)	170.3(3)
C(1)–Ir(1)–N(2)	80.1(3)	N(2)–Ir(1)–N(2A)	172.7(4)
C(1)–Ir(1)–N(2A)	94.9(3)	N(1)–Ir(1)–C(1A)	170.3(3)
C(1)–Ir(1)–C(1A)	94.5(4)		

shown in Figure 3. The coordination of the iridium atom is distorted octahedral, with the largest deviation represented by the bite angle of the bipyridine ligand at 76.3° (Table 1). The metalated C atoms of the ppy ligands are in a mutually *cis* arrangement, and their high *trans* influence leads to Ir–N(bpy) distances (2.151(6) Å) longer than the corresponding distances (2.015(7) Å) in the cyclometalated ligand. The two alkyl chains of the 4,4'-substituted bpy ligand are divergent and in an *all-trans* conformation.

In the crystal packing, the metal complex cations and PF_6^- anions are connected by weak C–H...F–P hydrogen bonds (Figure S1). The intra- and intermolecular C–H...F interactions involve aromatic C–H bonds from pyridine rings of both bpy and ppy ligands or aliphatic C–H bonds. The average H...F distance is 2.60 Å, a value that is in the high-end region reported

(37) Sprouse, S.; King, K. A.; Spellane, P. J.; Watts, R. J. *J. Am. Chem. Soc.* **1984**, *106*, 6647.

(38) Neve, F.; Crispini, A. *Eur. J. Inorg. Chem.* **2000**, 1039.

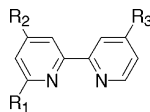
(39) van Diemen, J. H.; Haasnoot, J. G.; Hage, R.; Müller, E.; Reedijk, J. *Inorg. Chim. Acta* **1991**, *181*, 245.

(40) Urban, R.; Kramer, R.; Shahram, M.; Polborn, K.; Wagner, B.; Beck, W. *J. Organomet. Chem.* **1996**, *517*, 191.

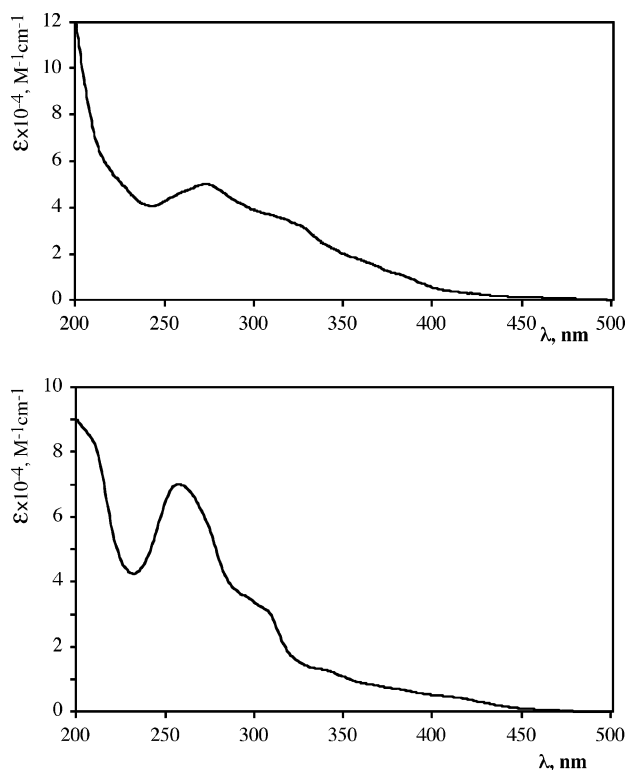
(41) Lo, K. K.-W.; Chung, C. K.; Lee, T. K.-M.; Lui, L.-H.; Tsang, K. H.-K.; Zhu, N. *Inorg. Chem.* **2003**, *42*, 6886.

(42) Kisko, J. L.; Barton, J. K. *Inorg. Chem.* **2000**, *39*, 4942.

(43) Ghizdavu, L.; Lentzen, O.; Schumm, S.; Brodtkorb, A.; Moucheron, C.; Kirsch-De Mesmaeker, A. *Inorg. Chem.* **2003**, *42*, 1935.

Table 2. Spectroscopic and Electrochemical Data for Complexes [Ir(ppy)₂(R,R'-bpy)]⁺ (1–5) in Acetonitrile Solution

complex	R ¹	bpy-ligand		absorption	redox potentials	
		R ²	R ³	λ_{\max}^c , nm (ϵ , M ⁻¹ cm ⁻¹)	E_{ox} , V vs SCE	$E_{\text{red}}^{1/2}$, V vs SCE
1	Ph	Ph-4-OR' (R' = <i>n</i> -C ₁₂ H ₂₅)	H	273 (52 380) 321sh (35 759)	+1.20 (q rev)	-1.38; -1.90 (irr)
2	Ph	Ph-4-OCOR' (R' = C ₆ H ₄ OCOC ₆ H ₄ OC ₆ H ₁₃)	H	268 (88 337)	+1.20 (q rev)	-1.28; -1.72 (irr)
3	Ph	Ph-4-COOR' (R' = Chol)	H	272 (56 299) 385sh (6 525)	+1.19 (q rev)	-1.32; -1.79 (irr)
4	H	C(O)OR' (R' = <i>n</i> -C ₁₆ H ₃₃)	C(O)OR'	270 (99 454) 375sh (11 715)	+1.30	-0.99; -1.54 (irr)
5	H	<i>n</i> -C ₉ H ₁₉	<i>n</i> -C ₉ H ₁₉	257 (70 100) 305sh (31 670) 338sh (13 070)	+1.24	-1.48

**Figure 4.** Absorption spectra of **1** (top) and **5** (bottom) in acetonitrile solution.

for significant C–H...F–P interactions involving organometallic cations and PF₆⁻ anions.⁴⁴

Absorption Spectra. The absorption spectra of all the compounds in acetonitrile fluid solution (Table 2, Figure 4) are dominated by intense bands at $\lambda < 300$ nm ($\epsilon > 50\,000$ M⁻¹ cm⁻¹) and by moderately intense bands at longer wavelengths which extend far within the visible region. The absorption at $\lambda < 300$ nm is mainly due to spin-allowed π – π^* ligand-centered (LC) transitions. In particular, on the basis of literature data,^{1b,45} the bands peaking in the 260–275 nm range receive larger contributions from ppy-centered transi-

tions, and absorption in the 275–300 nm range receives larger contributions from bpy-centered transitions. The absorption features in the range 300–450 nm are assigned to spin-allowed MLCT transitions, with the lowest energy one involving the substituted bpy ligand in all cases.

However, it should be considered that in Ir(III) cyclometalated compounds, as a consequence of the large covalency of the Ir–C⁻ bond, the use of a localized description of molecular orbitals, transitions, and states (the so-called localized molecular orbital approximation) is not as straightforward as in the case of metal complexes containing only polypyridine ligands. In fact, for several Ir(III) cyclometalated compounds it has been verified that the HOMO can be significantly delocalized over the cyclometalating ligands, with a large participation also from the Ir–C⁻ σ bond orbital.⁴⁶ Therefore, besides Ir-to-bpy MLCT transitions, even σ bond-to-ligand charge transfer transitions, or to simplify ppy-to-bpy charge transfer (LLCT) transitions, should contribute to the visible region CT bands. Finally, the absorption features at lowest energy in all the compounds ($\lambda > 450$ nm) are assigned to spin-forbidden CT transitions, which steal intensity from the spin-allowed transitions thanks to the large spin–orbit coupling induced by the heavy iridium center.

Redox Behavior. On oxidation, complexes **1–3** exhibit a quasi-reversible monoelectronic process at about +1.20 V vs SCE, whereas complexes **4** and **5** undergo a reversible monoelectronic process (Table 2, Figure 5). Oxidation processes in Ir(III) cyclometalated compounds have been assigned to metal-centered orbitals and/or to σ bond Ir–C⁻ orbitals.⁴⁶ It is assumed that pure metal-centered oxidations are reversible, and irreversibility increases as the contribution to the HOMO of the cyclometalating phenyl(s) increases.⁴⁷ On such a basis, one is led to assign the reversible oxidations of **4** and **5** to metal-centered processes and the quasi-reversible oxidation processes occurring in **1–3** to

(44) Grepioni, F.; Cojazzi, G.; Draper, S. M.; Scully, N.; Braga, D. *Organometallics* **1998**, *17*, 296.

(45) Juris, A.; Balzani, V.; Barigelletti, F.; Campagna, S.; Belser, P.; von Zelewsky, A. *Coord. Chem. Rev.* **1988**, *84*, 85.

(46) (a) Didier, P.; Ortmans, L.; Kirsch-De Mesmaeker, A.; Watts, R. *Inorg. Chem.* **1993**, *32*, 5239. (b) Serroni, S.; Juris, A.; Campagna, S.; Venturi, M.; Denti, G.; Balzani, V. *J. Am. Chem. Soc.* **1994**, *116*, 9086. (c) Polson, M.; Fracasso, S.; Bertolasi, V.; Ravaglia, M.; Scandola, F. *Inorg. Chem.* **2004**, *43*, 1950.

(47) Calogero, G.; Giuffrida, G.; Serroni, S.; Ricevuto, V.; Campagna, S. *Inorg. Chem.* **1995**, *34*, 541.

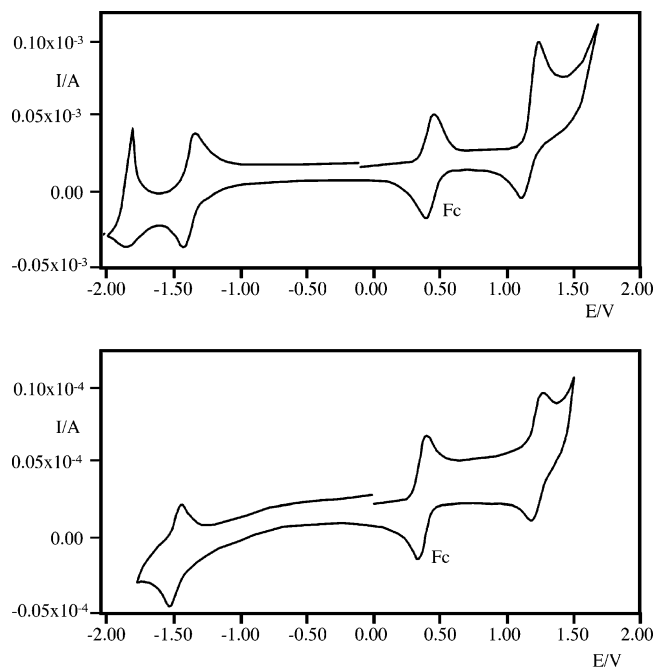


Figure 5. Differential pulse voltammograms of **1** (top) and **5** (bottom) in acetonitrile. Fc is ferrocene, used as an internal standard (see Experimental Section).

orbitals that are delocalized over the phenyl ligands. The difference in oxidation potentials between **4** and **5** is easily attributed to the different electron donor/acceptor abilities of the bpy ligands: the electron acceptor carboxyl groups of **4** stabilize the metal orbitals, leading to more positive oxidation potential for **4** compared to **5** (Table 2). However, this first-sight assignment suffers from an apparent contradiction. It is expected that as the Ir $d\pi$ orbitals are stabilized, their mixing with the phenyl orbitals increases and the σ bond orbitals are destabilized.⁴⁶ In other words, it is somewhat puzzling that **4** exhibits a reversible oxidation, metal-centered, at +1.30 V whereas **1–3** exhibit a σ bond-based quasi-reversible oxidation at +1.20 V. In fact, assuming our assignment of the oxidation process of **1–3** is correct, it is expected that the two strong electron-withdrawing ester groups of **4** would stabilize—as apparently they do—the metal-centered orbitals (and as a consequence destabilize the σ bond orbital) to a larger extent than substituents in **1–3**, thus pushing the σ bond orbital higher in energy than the metal-centered one.⁴⁸ Simply speaking, on the basis of the oxidation behavior of **1–3**, one would expect for **4** an irreversible process at a potential close to or less positive than +1.20 V. This apparent discrepancy can be solved if one assumes that another element may play a role in determining the oxidation potential of **1–3**. This element is the phenyl substituent in *ortho* position to the chelating bpy ligands of **1–3**. As revealed by the crystal structure of **3**,³⁸ as well as that of a related compound,³⁰ this phenyl ring is nearly parallel to one pyridine ring of a metalated ppy ligand, affording a heterogeneous intramolecular stack.⁴⁹ The ppy–phenyl stacking in-

teraction could therefore stabilize the positive charge delocalized on the ppy upon oxidation of the ppy-centered (or σ bond centered) orbital, thus shifting the oxidation potential of the latter to less positive values than the metal-centered oxidation process in **1–3**. Further support to the participation of the 6'-phenyl substituent of the polypyridine ligands in the oxidation processes of **1–3** comes from a comparison of our data and the luminescence data of literature compounds and will be discussed later. In conclusion, while the first oxidation processes of **4** and **5** are polypyridine ligand-based, the first oxidation processes of **1–3** are tentatively assigned to a very delocalized orbital with contributions from the mutually stacked pyridine ring (of one ppy ligand) and the 6'-phenyl substituent of the bpy subunit. For simplicity, herein we will continue to call it a ppy-centered orbital, but having in mind it is a rather peculiar one.

On reduction, the first process of each compound is assigned to bpy-centered orbitals, with potential values closely matching the electron acceptor/donor ability of the various substituents (Table 2). As far as the second reduction process is concerned, in complexes **1–3** it is assigned to ppy-centered orbitals, while in **4** it is attributed to the second reduction of the substituted bpy orbital. This assignment is based on the first reduction potential of other homoleptic cyclometalated complexes (whose reduction processes obviously involve cyclometalated ligands), which occur in the -1.70 – -2.00 V range.^{1b} The second reduction of **4**, on the contrary, is out of such potential range. Compound **5** does not undergo a second reduction process in the potential window investigated (< -2.00 V vs SCE). Most likely the presence of the donor substituents on the bpy ligand pushes reduction of the ppy ligands out of the window. In fact, ppy-based reduction in **5** is expected to be more negative than the second reduction of **1**, which takes place at -1.90 V (Table 2).

Luminescence Properties. All the compounds studied here exhibit luminescence in all the conditions investigated, that is, in acetonitrile fluid solution at room temperature, in rigid matrix at 77 K, and in solid film at room temperature. Luminescence decays were in all cases strictly monoexponential. Luminescence data are collected in Table 3, whereas luminescence spectra of some representative complexes are displayed in Figures 6 and 7.

For all the complexes, emission spectral shapes, energies, lifetimes, and quantum yields, as well as the dependence of the latter two properties on oxygen at room temperature, are indicative of emission properties due to triplet excited states having charge transfer character.^{1,45,46,50} Differences in emission energies of the compounds also agree with this assignment. The energy ordering indeed reflects the increasing electron acceptor ability of the different substituents on the bpy ligand, with emission energy decreasing in the order **5** > **1** > **2** > **3** > **4** (Table 3), in all the experimental conditions. The blue shift of the emission spectra going from room-temperature fluid solution to 77 K rigid matrix is also typical of CT states, for solvent reorganization is fast

(48) Even leaving aside the σ bond orbital hypothesis as developed by Kirsch-De Mesmaeker and Watts,^{46a} and considering the oxidation processes of **1–3** simply ppy-centered, it is not understandable in a first approximation why the ppy-centered oxidation occurs at potentials more positive than +1.30 V in **4**, if one neglects the effect of the 6'-phenyl in **1–3**.

(49) Hunter, C. A.; Lawson, K. R.; Perkins, J.; Urch, C. J. *J. Chem. Soc., Perkin Trans. 2* **2001**, 651. (b) Janiak, C. *J. Chem. Soc., Dalton Trans.* **2000**, 3885.

(50) Crosby, G. A. *Acc. Chem. Res.* **1975**, *8*, 231.

Table 3. Photophysical Data^a for Complexes 1–5

complex	luminescence					
	298 K ^a			77 K ^b		solid ^c (298 K)
	λ_{\max} , ^d nm	τ , ns	Φ	λ_{\max} , nm	τ , μ s	$\lambda_{\max}(\text{uncorr})$, ^d nm
1	622	145	0.059	527	3.25	576
		65 (air)	0.026 (air)			
2	632	135	0.040	534	3.08	584
		60 (air)	0.028 (air)			
3	651	119	0.058	546	3.21	608
		63 (air)	0.023 (air)			
4	688	117	0.016	607	2.8	630
		44 (air)	0.006 (air)			
5	589	475	0.200	508	4.5	552
		68 (air)	0.029 (air)			

^a Acetonitrile deoxygenated solutions (air-equilibrated data are given in parentheses). ^b Butyronitrile rigid matrix. ^c Spin-coated film. ^d Solid state values uncorrected for PMT response. The luminescence maxima in the other conditions are corrected.

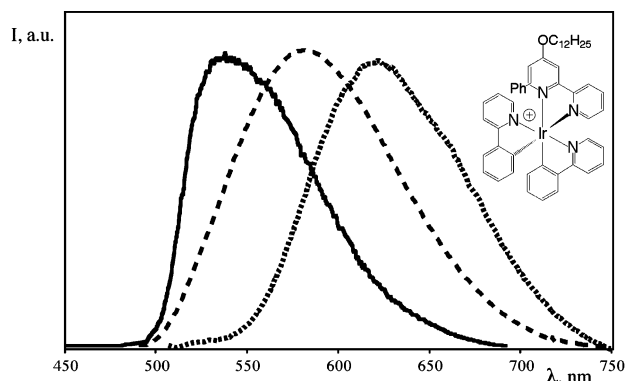


Figure 6. Luminescence spectra of **1**. Solid line: butyronitrile rigid matrix at 77 K; dashed line: spin-coated film, 298 K; dotted line: acetonitrile solution at 298 K. Spectra in fluid solution and at 77 K are corrected, while the spectrum of the spin-coated film is uncorrected for PMT response.

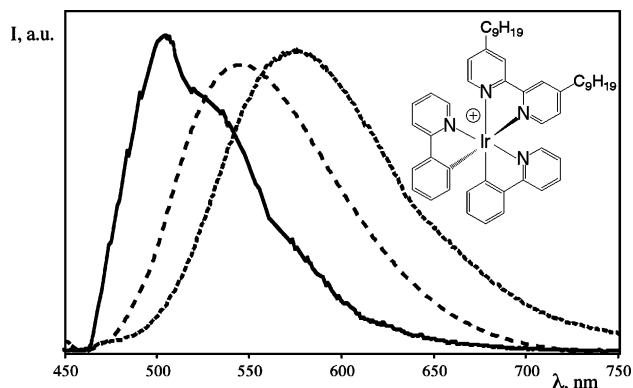


Figure 7. Luminescence spectra of **5**. Solid line: butyronitrile rigid matrix at 77 K; dashed line: spin-coated film, 298 K; dotted line: acetonitrile solution at 298 K. Spectra in fluid solution and at 77 K are corrected, while the spectrum of the spin-coated film is uncorrected for PMT response.

in fluid solution at room temperature and it stabilizes the CT states before emission takes place. This process is hampered at 77 K in a rigid matrix, and in this condition emission occurs from higher energy (Table 3).⁴⁵ The extent of the blue shift is related to the degree of real charge separation, that is, how much the charge distribution is different between ground and excited

states. For typical MLCT emitters, like the well-known $[\text{Ru}(\text{bpy})_3]^{2+}$ complex and analogous compounds, such a blue shift is usually in the range $1000\text{--}2000\text{ cm}^{-1}$, and it is also in the same range for Ir(III) cyclometalated compounds, which are reported to be pure MLCT emitters.^{1b,36,46a,51} However, energy separation between emission maxima in fluid solution at room temperature and in a rigid matrix at 77 K in **1–3** (around 2900 cm^{-1}) is very large for pure MLCT emitters. Also on the basis of the redox behavior (see above), we take this as an indication that the origin of the emitting level of **1–3** is not an MLCT state(s), but rather an LLCT (ppy-to-bpy) triplet state in which the donor orbital is the ppy-centered one discussed above. A relatively large inner and outer reorganization is expected to take place in such an excited state, and this would justify the large blue shift going from high to low temperature. It should be noted that recently Scandola and co-workers reported a bis-tridentate Ir(III) cyclometalated compound exhibiting a very small red shift of the emission band on passing from low to high temperature, still assigning the emission to a triplet LLCT state.^{46c} However in their case the charge redistribution in the excited state compared to the ground state was also very small, due to the particular nature of the ligands involved. This suggests that whereas in general the extent of red shift in emission for pure MLCT states is in some way similar in all the complexes, it can be quite different for LLCT emitters, strongly depending on the specific case.

A further indication in favor of the particular nature of the LLCT emission (and as a consequence of the unusual nature and potential value of the first oxidation process) of **1–3** comes from the comparison between the room-temperature emission of a formerly studied compound like **1–3**, i.e., $[\text{Ir}(\text{ppy})_2(\text{L})]^+$ (where $\text{L} = 4'-(4''\text{-chlorophenyl})-6'\text{-phenyl}-2,2'\text{-bipyridine}$)³⁰ and $[\text{Ir}(\text{ppy})_2(\text{bpy-Ph-4-Br})]^+$ (where $\text{bpy-Ph-4-Br} = 4'-(4''\text{-bromophenyl})-2,2'\text{-bipyridine}$).³⁶ While emission from the former species was originally attributed to MLCT states, in light of the present discussion it should be more carefully assigned to an LLCT state as suggested for **1–3**. On the other hand, emission of $[\text{Ir}(\text{ppy})_2(\text{bpy-Ph-4-Br})]^+$ has been assigned to an MLCT triplet level. The main difference between the two compounds (leaving aside the less relevant difference between the halide substituents) is the presence of the 6'-phenyl ring in the backbone of the L ligand in $[\text{Ir}(\text{ppy})_2(\text{L})]^+$. While $[\text{Ir}(\text{ppy})_2(\text{bpy-Ph-4-Br})]^+$ in acetonitrile emits with a maximum at 611 nm, in the same medium the emission maximum for $[\text{Ir}(\text{ppy})_2(\text{L})]^+$ is reported at 645 nm. Such a large emission energy difference is hardly attributable only to the electron-withdrawing effect of the 6'-phenyl on the bpy-like ligand L. Yet it fits quite well with the hypothesis that the 6'-phenyl substituent may stabilize the oxidation of the stacked ppy and, as a consequence, the corresponding LLCT state.

As far as luminescence of **4** and **5** is concerned, it is interesting to note that the blue shift on passing from fluid solution at room temperature to rigid matrix at 77 K is less than 2000 cm^{-1} (Table 3). This was indeed expected since these species should be almost pure MLCT emitters. Emission differences, such as excited

(51) Colombo, M. G.; Hauser, A.; Gudiel, H. U. *Inorg. Chem.* **1993**, *32*, 3088.

state energy, lifetime, and quantum yields, between these two species are related to the difference mainly in (metal-centered) oxidation and (bpy-centered) reduction potentials (Table 2) and to the energy gap law.

The solid film luminescence warrants a final comment. Obviously, in the perspective of using Ir(III) cyclometalated species as components of electroluminescent devices, solid state emission properties are quite important. Therefore, it is of interest to foresee intermolecular interactions in the solid state which could "poison" the useful excited state properties. The species here investigated exhibit emission in spin-coated films (Table 3). Interestingly, the solid emission maxima are intermediate between those in a rigid matrix and in fluid solution, with the same emission energy ordering found at room temperature and at 77 K. This suggests that the same attribution of the emission as LLCT (1–3) or MLCT (4, 5) in nature also holds in this experimental condition, whereas no formation of exciplexes or excimers is revealed. However, we cannot definitely exclude some excited state quenching through intermolecular interaction, although the long tails of the bpy-like ligands should inhibit these effects, as demonstrated for dendrimerized Ir(III) complexes.⁹ Finally, it should be noted that for technical reasons it was impossible to correct the film luminescence spectra for PMT response. Nevertheless, taking into account the shape of the uncorrected spectra and the photomultiplier response profile, the corrected emission maxima of the film spectra are expected to be red-shifted by no more than 20 nm from the uncorrected values, so that the conclusion that solid state emission spectra of the complexes are intermediate in energy between fluid solution and 77 K matrix emission spectra, as reported above, keeps its validity.

Conclusions

We have investigated the absorption spectra, redox behavior, and photophysical properties (in fluid solution and in films at room temperature and in a rigid matrix at 77 K) of five Ir(III) cyclometalated compounds of general formula $[\text{Ir}(\text{ppy})_2(\text{R},\text{R}'\text{-bpy})]^+$, including two species here synthesized and structurally characterized for the first time. All the species exhibit strong absorption in the UV region, due to spin-allowed LC transitions, and moderately intense bands in the visible region, due to CT transitions. Several redox processes have been evidenced in each complex and assigned to specific components. All the species also exhibit relatively strong and long-lived (from 10^{-8} to 10^{-5} s, depending on temperature and matrix) luminescence. The substituents of the polypyridine ligands affect in a substantial way the spectroscopic, redox, and photophysical properties of the compounds. In particular, a phenyl substituent on the polypyridine chelating ligand in the 6' position stabilizes oxidation of an orbital which receives significant contributions from the cyclometalated ppy ligands and leads to emission from triplet LLCT excited states. When such a phenyl is absent in the R,R'-bpy ligand structure, the usual triplet MLCT emission predominates.

Experimental Section

All reactions were carried out in air. Reagent grade solvents and ammonium hexafluorophosphate from Aldrich were used

as received. The ligand 4,4'-di-*n*-nonyl-2,2'-bipyridine (97%) was purchased from Aldrich. The ligand 4,4'-di-hexadecyloxy-carbonyl-2,2'-bipyridine⁵² and the complex $[\text{Ir}(\text{ppy})_2\text{Cl}]_2$ ³⁷ were prepared according to literature methods.

The synthesis of complexes 1–3 was reported previously.³⁸ The preparation of complexes 4 and 5 was carried out in a similar manner. A typical preparation is reported for complex 4. All species 1–5 are air-stable solids with high solubility in common organic solvents such as acetone, acetonitrile, and chlorinated solvents.

Bis(2-phenylpyridine-*C*²,*N*¹')(4,4'-dihexadecyloxy-carbonyl-2,2'-bipyridine) iridium(III) Hexafluorophosphate (4). A stirred suspension of $[\text{Ir}(\text{ppy})_2\text{Cl}]_2$ (0.08 g, 0.075 mmol) and 4,4'-di-hexadecyloxy-carbonyl-2,2'-bipyridine (0.10 g, 0.150 mmol) in CH_2Cl_2 –MeOH (15 mL, 2:1 v/v) was heated to reflux. After 45 min the resulting dark red solution was cooled to room temperature. The addition of a 5-fold excess of ammonium hexafluorophosphate dissolved in MeOH (1 mL) followed by stirring for 30 min did not cause any further color change. The solution was evaporated to dryness under reduced pressure, affording a red crude solid. The solid was redissolved with 10 mL of CH_2Cl_2 and filtered to remove insoluble white inorganic salts. Diethyl ether was layered onto the red filtrate, and the mixture was cooled to $\sim 4^\circ\text{C}$. Red-orange plates of the desired product formed overnight. Yield: 0.130 g (63%). Mp > 200 °C. IR (KBr, cm^{-1}): 1732 (COO); 839 (PF_6^-). ¹H NMR (CDCl_3 , 300 MHz): δ 9.01 (s, 1H), 8.13 (d, 1H, $J = 5.5$ Hz), 8.00 (d, 1H, $J = 5.5$ Hz), 7.90 (d, 1H, $J = 8.1$ Hz), 7.76 (t, 1H, $J = 7.7$ Hz), 7.69 (d, 1H, $J = 7.7$ Hz), 7.57 (d, 1H, $J = 5.5$ Hz), 7.10 (t, 1H, $J = 6.4$ Hz), 7.06 (t, 1H, $J = 7.3$ Hz), 6.94 (t, 1H, $J = 7.3$ Hz), 6.28 (d, 1H, $J = 7.3$ Hz), 4.42 (t, 2H, $J = 6.8$ Hz), 1.80 (m, 2H), 1.42–1.18 (m, 26H). 0.88 (t, 3H, $J = 6.6$ Hz). MS (MALDI-TOF/TOF, α -CHCA, CH_3CN): m/z 1193.9 (M – PF_6). Anal. Calcd for $\text{C}_{66}\text{H}_{88}\text{F}_6\text{IrN}_4\text{O}_4\text{P}$: C, 59.22; H, 6.63; N, 4.19. Found: C, 59.33; H, 6.32; N, 4.60.

Bis(2-phenylpyridine-*C*²,*N*¹')(4,4'-di-*n*-nonyl-2,2'-bipyridine) iridium(III) Hexafluorophosphate (5). Yellow microcrystalline solid. Yield: 75%. Mp > 200 °C. IR (KBr, cm^{-1}): 837 (PF_6^-). ¹H NMR (CDCl_3 , 300 MHz): δ 8.45 (s, 1H), 7.92 (d, 1H, $J = 8.1$ Hz), 7.79 (d, 1H, $J = 5.7$ Hz), 7.78 (dt, 1H, $J = 7.8, 1.4$ Hz), 7.69 (d, 1H, $J = 7.5$ Hz), 7.56 (d, 1H, $J = 5.6$ Hz), 7.21 (d, 1H, $J = 5.2$ Hz), 7.07 (t, 1H, $J = 7.3$ Hz), 7.05 (t, 1H, $J = 7.8$ Hz), 6.92 (t, 1H, $J = 7.3$ Hz), 6.32 (d, 1H, $J = 7.3$ Hz), 2.89 (t, 2H, $J = 7.5$ Hz), 1.72 (m, 2H), 1.38–1.22 (m, 12H), 0.89 (t, 3H, $J = 6.7$ Hz). MS (MALDI-TOF/TOF, α -CHCA, CH_3CN): m/z 909.6 (M – PF_6). Anal. Calcd for $\text{C}_{50}\text{H}_{60}\text{F}_6\text{IrN}_4\text{P}$: C, 56.97; H, 5.74; N, 5.31. Found: C, 56.75; H, 5.81; N, 5.06.

Measurements. ¹H NMR spectra were recorded at 300.13 MHz with a Bruker AC 300 spectrometer with internal TMS reference. FT-IR spectra were recorded on a Perkin-Elmer 2000 spectrophotometer for KBr pellets. Elemental analyses were performed using a Perkin-Elmer 2400 microanalyzer. All mass spectra were recorded on a 4700 Proteomics analyzer with TOF/TOF optics (Applied Biosystems). This MALDI tandem mass spectrometer uses a 200 Hz frequency-tripled Nd:YAG laser operating at 4700. Averages of 5000 laser shots were used to obtain the MS spectra.

Electrochemical measurements were carried out in argon-purged acetonitrile at room temperature with a PAR 273 multipurpose apparatus interfaced to a PC. The working electrode was a glassy carbon (8 mm², Amel) electrode. The counter electrode was a Pt wire, and the reference electrode was a SCE separated with a fine glass frit. The concentration of the complexes was about 5×10^{-4} M. Tetrabutylammonium hexafluorophosphate was used as supporting electrolyte, and its concentration was 0.05 M. Cyclic voltammograms were obtained at scan rates of 20, 50, 200, and 500 mV/s. For reversible processes, half-wave potentials (vs SCE) were

(52) Pucci, D.; Barberio, G.; Crispini, A.; Ghedini, M.; Francescangeli, O. *Mol. Cryst. Liq. Cryst.* **2003**, *395*, 325.

calculated as an average of the cathodic and anodic peaks. The criteria for reversibility were the separation between cathodic and anodic peaks, the close-to-unity ratio of the intensities of the cathodic and anodic currents, and the constancy of the peak potential on changing scan rate. For irreversible processes, the values reported in Table 2 are the peak estimated by differential pulse voltammetry (DPV). The number of exchanged electrons was measured with differential pulse voltammetry (DPV) experiments performed with a scan rate of 20 mV/s, a pulse height of 75 mV, and a duration of 40 ms. Absorption spectra were recorded with a Jasco 570 spectrophotometer. Luminescence spectra were performed with a Jobin-Yvon Fluoromax 2 spectrofluorimeter equipped with a Hamamatsu R928 photomultiplier and were corrected for photomultiplier response by using a standard lamp. Emission lifetimes were measured with an Edinburgh OB900 single-photon-counting apparatus (nitrogen discharge; pulse width, 3 ns). Emission quantum yields were measured at room temperature (25 °C) with the optically dilute method,⁵³ calibrating the spectrofluorimeter with a standard lamp. [Ru(bpy)₃]²⁺ in aerated aqueous solution was used as a quantum yield standard, assuming a value of 0.028.⁵⁴ Experimental uncertainties are as follows: redox potentials, ±10 mV; absorption maxima, 2 nm; extinction coefficients, 10%; emission maxima, 4 nm; emission lifetimes, 10%; emission quantum yields, 20%.

X-ray Structural Determination of 5. A yellow plate (0.16 × 0.20 × 0.04 mm) was selected among single crystals obtained directly from the mixture layered with ether and cooled to 4 °C. Diffraction data were collected at 100 K on a Bruker-Nonius X8 Apex CCD area detector equipped with graphite monochromator and Mo K α radiation ($\lambda = 0.71073$) and Cryostream (Oxford Cryosystems) open-flow N₂ cryostats. The crystal was mounted with Paratone-N oil (Hampton Research) coating. The crystal-to-detector distance was

4.01 cm. The unit cell parameters were determined from three frames, then refined on all data. A series of frames were recorded using a multiscan method (both ω and ϕ scans) to ensure that a complete and redundant dataset was collected up to θ of 26.4. Data reduction was performed using SAINT programs; absorption corrections based on multiscan were applied using SADABS.⁵⁵ Crystallographic data and data collection parameters are summarized in Table S1.

Since it was not possible to distinguish between the *Cc* and *C2/c* space groups from the analysis of the systematic absences, attempts to solve the structure in both acentric and centric systems (both by direct methods) were made. The best solution was found in the *C2/c* space group. Full matrix least squares refinements on F^2 were carried out using SHELXL-97 (SHELXTL-NT software package)⁵⁶ with anisotropic displacement parameters for all non-hydrogen atoms. All H atoms were placed in calculated positions and in riding modes.

Acknowledgment. We thank Dr. Anna Napoli for the MALDI-TOF mass spectra and Prof. Daniela Pucci for a sample gift of the ligand 4,4'-dihexadecyloxy-carbonyl-2,2'-bipyridine. Financial support from the Ministero dell'Istruzione, dell'Università e della Ricerca (MIUR), is gratefully acknowledged.

Supporting Information Available: Crystal packing (Figure S1), crystallographic data and refinement parameters (Table S1), and X-ray crystallographic file in CIF format for compound 5. This material is available free of charge via the Internet at <http://pubs.acs.org>.

OM049493X

(55) SMART, SAINT, and SADABS; Bruker AXS, Inc.: Madison, WI, 1997.

(56) SHELXTL-NT Crystal Structure Analysis Package, Version 5.1; Bruker AXS Inc.: Madison, WI, 1999.

(53) Demas, J. N.; Crosby, G. A. *J. Phys. Chem.* **1971**, *75*, 991.

(54) Nakamaru, K. *Bull. Chem. Soc. Jpn.* **1982**, *55*, 2697.